

Original Article

A Computerized Approach for Emotion Recognition from EEG Signals Using Gazelle-Whale Optimization and Attention-Based Improved DCNN-BILSTM

T. Manoj Prasath¹, R. Vasuki²

^{1,2}Department of Biomedical Engineering, Bharath Institute of Higher Education and Research, Tamilnadu, India.

¹Corresponding Author : manojprasath@gmail.com

Received: 11 January 2024

Revised: 08 February 2024

Accepted: 09 March 2024

Published: 25 March 2024

Abstract - The use of Electroencephalogram (EEG) signals for emotion recognition has demonstrated remarkable success across diverse fields such as medicine, security, and human-computer interaction. Recent advancements in Deep Learning (DL) techniques have substantially enhanced classification precision compared to traditional signal processing and Machine Learning (ML) approaches. This work focuses on developing a computerized methodology to effectively recognize emotions from EEG signals, emphasizing the crucial processes of feature extraction, feature selection and emotion classification. Traditional approaches in emotion recognition from EEG signals face challenges in achieving high accuracy. The motivation behind this work is to harness the benefits of Deep Learning (DL) for optimal emotion recognition. The proposed methodology aims to address existing limitations and improve the efficacy of emotion recognition systems. Gaussian smoothing filters are applied to the EEG brainwave dataset to reduce artifacts, ensuring a cleaner input for subsequent processing. Features are extracted using Empirical Mode Decomposition (EMD), providing enhanced spatial accuracy and temporal resolution in representing emotional states. A hybrid Gazelle-Whale Optimization approach is employed to select optimal features, improving the efficiency of subsequent classification stages. Attention-based Improved Deep Convolutional Neural Network (DCNN) coupled with Bidirectional Long Short-Term Memory (Bi-LSTM) networks is utilized for accurate emotion classification. This combination integrates the strengths of DL in capturing intricate patterns within EEG signals. The integrated deep learning techniques and optimization strategies lead to more accurate and reliable emotional state classifications. The outcomes for the proposed topology demonstrate a high accuracy of 98.28%, F1 score of 97.54%, recall measuring 98.28% and precision scoring of 98.12%, respectively.

Keywords - Electroencephalogram, Empirical Mode Decomposition, Gazelle-Whale Optimization (GWO), DCNN- Bi-LSTM, Gaussian smoothing filters.

1. Introduction

The brain-computer interface is one area of human-computer interaction that enables the connection between the human brain and electrical devices like computers and smartphones. The device, which uses a range of signals, including EEG signals, can be communicated with the user using a BCI system.

Comprehending the objectives of brain signals and converting them into actions is the primary aim of the several processing phases in the BCI center [1]. BCI techniques get brain signals from a subject, examine the data they contain, and utilize the results to determine what could have caused the signal-generating behavior. In non-medical contexts such as games, entertainment, education, and monitoring, EEG signals are widely used [2]. The process of understanding and identifying a person's current mental state or state of mind is

known as emotion recognition. In current years, considerable research has been done on the recognition of emotions from brain signals [3, 4]. In reality, multiple EEG signals are usually used for emotion identification to study the dynamic oscillations of the brain. The EEG-based emotion detection system performs several EEG signal preprocessing steps, such as channel, time segment, and frequency band selection, to reduce noise in EEG data and improve signal quality [5-7].

To remove noise from the EEG signals, the traditional methods included a variety of filtering techniques, including the kernel filter [8], median filter [9], and Kalman filter [10]. Nevertheless, the signal noise is not effectively eliminated when employing those filters [11]. The present research now incorporates the sophisticated Gaussian smoothing Filter, which provides remarkable flexibility in balancing eliminating undesired interference and preserving relevant



emotional information. The main tasks involve identifying emotionally significant features from various sources and analyzing feature sets to remove redundant or irrelevant features. [12]. A feature selection model's primary objective is to select the optimal features to reduce processing time while boosting accuracy during classification. This is accomplished, and classification accuracy is increased by using optimization methods to eliminate extraneous features from the initial feature vector [13, 14].

FS models have been effectively applied by researchers in many different fields. However, finding significant discriminative traits is still a challenging task [15]. Because of its straightforward computation, Otsu's method is among the finest for image thresholding; nonetheless, segmentation issues may arise if the histogram stops being bimodal.

Even though K-means performs best when the data set is distinct, selecting the number of cluster centers is essential for the learning process [16]. The process known as Linear Discriminant Analysis (LDA) is straightforward, efficient, and portable. To minimize the amount of features and handle the problem of overfitting data, the Principal Component Analysis (PCA) method is introduced.

Compared to conventional DWT processes, the Empirical Mode Decomposition feature extraction approach greatly reduces the time required to compress images when converting RGB to grayscale [17]. Techniques such as Adaptive Auto Regressive parameters (AAR) [18] and Wavelet Packet Decomposition (WPD) [19] are used to extract features from EEG data. However, these methods fail

in every application due to their poor time localization, and it is hard to determine the properties of the representation for non-stationary signals like EEG signals.

Consequently, this work proposes using DCNN in conjunction with a hybrid Gazelle-Whale Optimization approach to select desired features effectively. A variety of classifiers are used to divide the signals into multiple categories. Classifiers for EEG-based emotion identification include CNN [1], Support Vector Machine (SVM) [20], Nearest Neighbor classifiers, and nonlinear Bayesian classifiers. It cannot, however, provide an accurate estimate for a sufficient category likelihood due to its complexity. An attention-based Improved DCNN-BiLSTM classifier is used to address the aforementioned issues. Additionally, it is used to expand the capabilities of the linear framework to infer human emotions from brain data.

2. Description of Proposed System

Brain waves reveal a person's emotional spectrum, and the EEG is the foremost hopeful instrument for recording these waves. The proposed work uses a hybrid Gazelle-Whale Optimization technique to identify an individual's hybrid DCNN-BiLSTM emotions for categorization to select better features. The workflow of the developed system is shown in Figure 1.

The EEG brainwave dataset is initially preprocessed to eliminate noise and interruptions from the input signal. The preprocessing used in the present research uses a Gaussian smoothing filter that provides balancing removal of unwanted interference with the preservation of relevant emotional data.

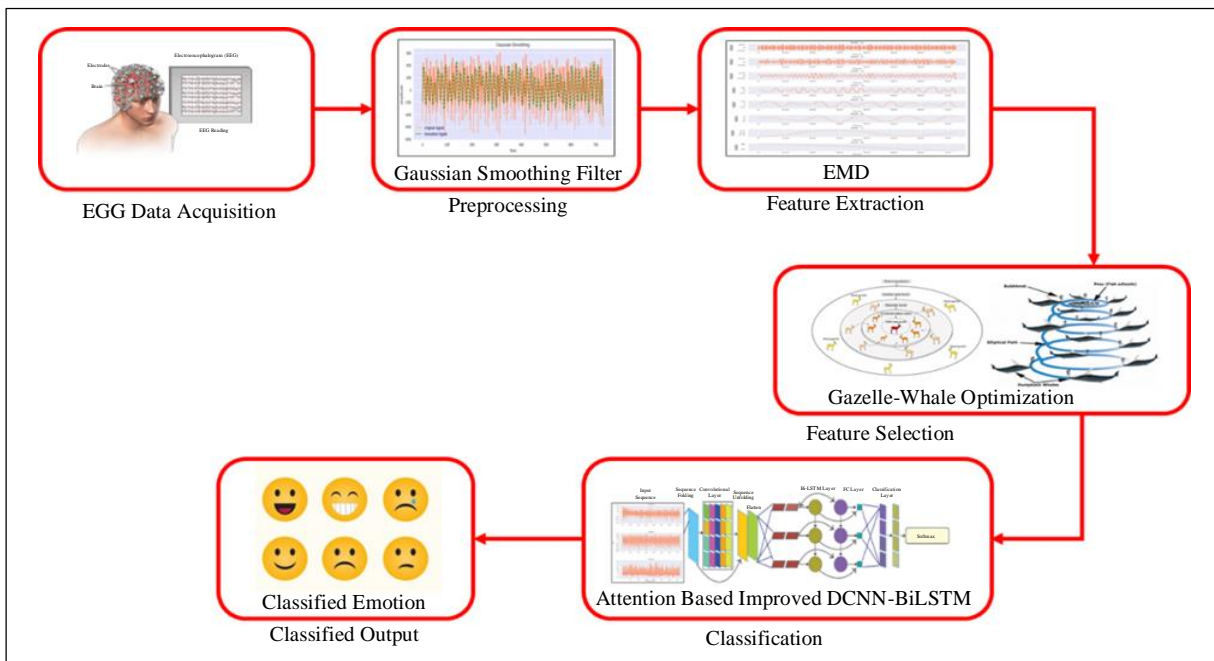


Fig. 1 Flow chart of proposed system

After preprocessing, EMD feature extraction is executed, which helps to extract complex, non-stationary features from EEG brainwave data and capture time-frequency representations. The best characteristics are chosen by incorporating the hybrid Gazelle-Whale optimization technique after extracting pertinent features. This combination refines the feature set by keeping only the features most effective at classifying emotions. Lastly, Hybrid Attention-based Improved DCNN-linked Bi-LSTM completes the classification task. By adding attention mechanisms, the network's capacity to concentrate on salient characteristics is further enhanced, resulting in an overall improvement in recognition performance. Performance indicators are used to gauge the model's overall efficacy.

3. System Modelling

3.1. Preprocessing by Gaussian Smoothing Filter

It has been demonstrated that the Gaussian Smoothing Filter (GSF) offers good filtering performance for a variety of applications, including object area filtering in pictures and filtering robot signals. The primary justifications for using GSF in various uses include:

- Easy to implement and performs well because it only has one defining parameter, making it possible to apply GSF with appropriate effort.
- The capacity to comprehend and forecast GSF behavior on EMG signals in both the frequency and temporal domains is made simple and easy by the similarity of supports in both domains.
- Its Gaussian form aids in striking a balance between removing noises and preserving some of the high-frequency components of the detected EMG signals.

In order to illustrate the three primary characteristics that a GSF may display, let's begin with the characteristic impulse response of a GSF, which can be explained by,

$$g(x_s(t)) = \frac{\exp\left(-\frac{(x_s(t))^2}{2\sigma^2}\right)}{\sqrt{2\pi\sigma^2}} \quad (1)$$

$x_s(t)$ is the detected EMG signal that needs to be smoothed, and σ is the GSF standard deviation. Given Equation 1, it is evident that the GSF has only one defining parameter, σ , making it a simple filter in its execution. The convolution operation of the GSF's impulse response, provided in Equation 1, can be used to detect EMG signals to estimate the component of $x_s(t)$ that corresponds to muscle contractions, or $x(t)$, using the GSF this results in:

$$\hat{x}(t) = x_s(t) * (x_s(t)) \quad (2)$$

Where $*$ indicates the convolution operator and $\hat{x}(t)$ is the estimated value of $x(t)$. It is then possible to rewrite Equation 2 using the convolution integral.

$$\hat{x}(t) = \int_{-\infty}^{\infty} x_s(\tau) g(x_s(t - \tau)) d\tau \quad (3)$$

The GSF's impulse response and using the Fourier transform to get Equation 1, we get,

$$G(f) = \exp(-2\pi^2 f^2 \sigma^2) \quad (4)$$

In this case, f stands for frequency. Equation 4, which is likewise a Gaussian function, shows that the GSF's temporal and frequency domain responses have a similar Gaussian function support. Although a GSF functions similarly to a Low-Pass Filter (LPF), its Gaussian function offers a reasonable balance between minimizing potential signal distortions during the filtering process and maintaining some of the high-frequency components of the original signal. As a result, it is shown that the GSF offers effective filtering performance, is straightforward to implement, supports similarities in both the time and frequency domains, and strikes a balance between filtering and maintaining the signal's high-frequency components.

3.2. Feature Extraction by EMD

The process of breaking down a non-stationary signal into a group of AM/FM nanocomponent signals is known as EMD. Intrinsic Mode Functions (IMFs) are the name given to these signals with a single component. The IMFs are extracted using an envelope subtraction method, and all derived findings are linearly combined into the original signal.

The indication is time-domain decomposed, maintaining the signal's fluctuating frequency and amplitude. Unlike the Fourier transform, EMD does not require an a-priority-defined basis function for the computation of IMFs. While EMD relies on the oscillation in the signal, the Fourier transform takes advantage of the signal's harmonic components.

Local maxima and minima in the signal are analyzed. Cubic spline is employed to determine the upper and lower envelopes using the knowledge about local peaks and minima. The typical envelope is produced utilizing the signal's trend, as indicated by the upper and lower envelopes. An IMF candidate is obtained by subtracting this mean envelope from the original signal. Before classifying this candidate as a genuine IMF, a test is run to see if there is a difference of no more than one between the number of zero crossings and the number of extrema.

The candidate is counted as an IMF, and the counter is increased if they meet the requirements; if not, the counter is reset to zero. Verification is done for every IMF created to see the requirements. The sorting procedure is repeated until the requirements are met if the criteria are not met. After that, the obtained IMF is saved and deducted from the initial indication to begin a fresh screening procedure for an additional IMF. Until the signal is deconstructed to the point where it contains no more than two extrema, the process is repeated.

3.2.1. Sifting Process for IMFs

Simplified, the EMD method can be described as a filter that sorts through the input and separates it into the mono-component signals (IMFs) mentioned above. When a function meets these requirements, it is referred to as an intrinsic mode function.

1. Identify extrema: Find all the local maxima and minima in the signal. These are points where the signal changes direction.
2. Interpolate envelopes: Connect the local maxima and minima with cubic spline interpolation to form upper and lower envelopes. These envelopes define the upper and lower bounds of the first IMF.
3. Calculate mean: Compute the average of upper and lower envelopes to get a mean envelope.
4. Extract IMF: Subtract the mean envelope from the original signal to obtain the first IMF. This IMF represents the highest frequency oscillation in the data.
5. Check for IMF criteria: Check whether the extracted IMF satisfies the IMF criteria, which include the number of extrema and zero crossings. If the criteria are not met, repeat steps 2-4 until convergence.
6. Repeat for residue: After extracting the first IMF, subtract it from the original signal to obtain a residue. Repeat steps 1-5 on the residue to extract subsequent IMFs.
7. Termination: Continue the sifting process until either the residue becomes a monotonic function or satisfies a stopping criterion.
8. Finalize IMFs: The IMFs obtained from the sifting process are the intrinsic mode functions of the signal.

It's significant to note that the sifting process is iterative, and each iteration refines the extracted IMFs by removing the high-frequency components from the signal. This process continues until the residue becomes a monotonic function or meets the stopping criterion, indicating that all relevant oscillatory modes have been extracted.

3.3. Selection of Features by Hybrid Gazelle-Whale Optimization

A hybrid Gazelle-Whale Optimization approach is employed for optimal feature selection. This hybrid optimization strategy aims to improve efficiency by leveraging the strengths of both GOA and WOA for subsequent classification stages by choosing the most pertinent features. At the beginning of the optimization process, a population of potential feature subsets is initialized using the Gazelle Optimization Algorithm (GOA). Each solution in the population is denoted as a binary vector, where each bit resembles the presence (1) or absence (0) of a particular feature. This initialization creates a diverse set of potential solutions to start the optimization.

$$X_{ij} = \{0,1\}, i = 1,2, \dots, N, j = 1,2, \dots, D \quad (5)$$

Where N refers to the population size, D specifies the number of features as well as X_{ij} represents the presence (1) or absence (0) of feature j in solution i .

During the exploitation phase, the algorithm simulates the grazing behavior of gazelles using Brownian motion.

$$X_{ij} = rand * (UB_j - LB_j) + LB_j \quad (6)$$

In every iteration, a potential location is determined for each X_{ij} utilizing a random number represented by 'rand'. The upper bound UB_j and lower bound LB_j constraints of the specified search space guide this determination. Brownian motion is a stochastic process that models the random movement of particles. In the context of feature selection, this motion is applied to explore the feature space efficiently. Each potential feature subset undergoes small, random changes to explore the neighborhood in the solution space.

$$f_B(x; \mu, \sigma) = \frac{1}{\sqrt{2\mu\sigma^2}} \exp\left(-\frac{(x-\mu)^2}{2\sigma^2}\right) = \frac{1}{\sqrt{2\mu}} \exp\left(-\frac{x^2}{2}\right) \quad (7)$$

Where $\mu = 0$ and $\sigma^2 = 1$. The fitness of each potential feature subset is evaluated based on a relevant evaluation metric, considering the performance of the associated machine learning model.

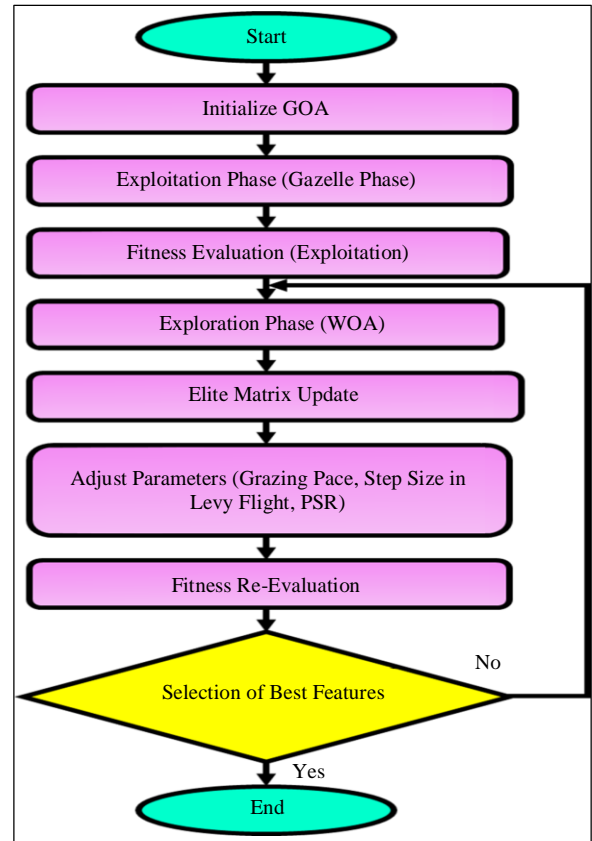


Fig. 2 Flowchart for the hybrid Gazelle-Whale Optimization

The exploration phase is introduced when faced with a “predator” situation, which could be a feature subset that does not perform well according to the evaluation metric. Inspired by the Whale Optimization Algorithm (WOA), this phase utilizes.

$$\vec{D} = \left| \vec{C} \cdot \vec{S}^{best}(i) - \vec{S}(i) \right| \quad (8)$$

$$\vec{S}(i + 1) = \vec{S}^{best}(i) - \vec{A} \cdot \vec{D} \quad (9)$$

Where $\vec{S}^{best}(i)$ represented optimal solution, $\vec{S}(i)$ denoted candidate solution at the current generation, and i indicates the current solution. Levy flight is introduced to perform random jumps and explore alternative feature subsets more extensively. Levy flight introduces long jumps that help escape local optima and search for more promising solutions in the solution space.

$$f_L(x; \alpha, v) = \frac{1}{n} \int_{-\infty}^0 \exp(-vq^\alpha) \cos(qx) \delta q \quad (10)$$

The algorithm employs the Levy flight as a strategy to move away from regions of the feature space that may lead to suboptimal solutions. An elite matrix is maintained, similar to the one used in the Gazelle Optimization Algorithm (GOA). This matrix represents the best-obtained feature subsets from both the exploitation and exploration phases. It guides the optimization process by incorporating successful features from previous iterations, ensuring that valuable information is retained and used to guide subsequent searches.

$$Elite_{ij} = \begin{cases} X_{ij} & \text{if the fitness of the new subset is better} \\ Elite_{ij} & \text{otherwise} \end{cases} \quad (11)$$

If a newly discovered feature subset outperforms the current elite, it replaces the elite; otherwise, the elite remains. The algorithm dynamically adjusts parameters such as grazing

pace (D), step size in the Levy flight (μ), and Predator Success Rates (PSRs) to balance the exploration and exploitation trade-off. This adaptability confirms that this algorithm responds effectively to different feature space characteristics and problem instances.

The fitness of each potential feature subset is reevaluated based on the performance of an ML model trained with selected features. This evaluation helps identify feature subsets that contribute to improved model performance. The best-performing feature subsets are selected and retained for subsequent iterations, ensuring that successful features from both exploitation and exploration phases are incorporated into the evolving solution space.

3.4. Classification by Improved DCNN-Bi-LSTM

Neural networks trained at different abstraction levels have many processing layers thanks to deep learning. Low-level characteristics are adaptively learned by the network from raw input, while high-level features are learned from low-level features using a ranking system. Two significant network types created as deep learning architectures are feed-forward networks and recurrent networks. The CNN is thought of in relation to feed-forward networks, and the LSTM is thought of in relation to recurrent networks.

The automatic categorization features in the optimal approach serve as the main keystone for addressing the power quality disturbance, and the focus is on developing a deep learning architecture for accurate disturbance classification and detection using a unique closed-loop feedback neural network. In order to minimize overfitting, it typically consists of a unit-based layer function with a one-dimensional convolutional layer, a max pooling layer, and a batch normalization layer model for advanced feature extraction from the disturbance. The proposed deep convolution neural network extracts detailed features automatically from a big raw dataset that is collected from a variety of samples using a stacked structure made up of multiple layers of units.

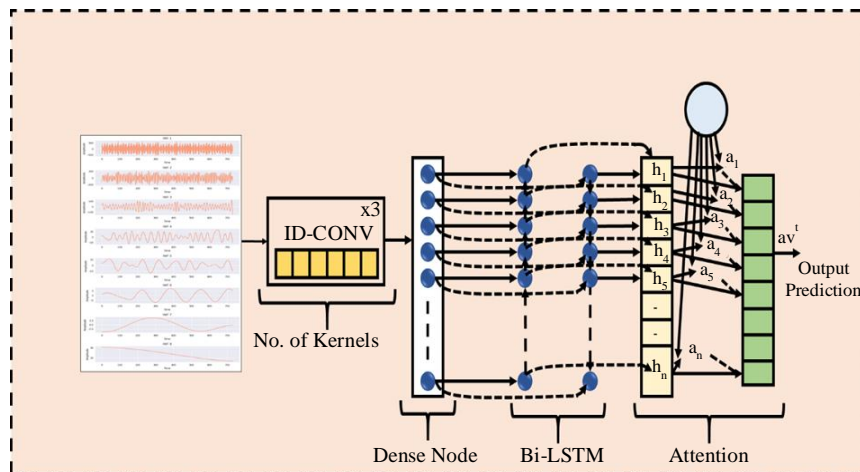


Fig. 3 Structure of improved DCNN-BiLSTM

3.4.1. Convolutional Neural Network

Deep learning is a machine learning approach that uses several processing layers to learn about input characteristics. Because of its superior performance in areas like visual object recognition and categorization, its popularity has recently surged. CNN deviates from traditional neural networks by displaying convolution feature extraction and classification features. Convolution, pooling, normalizing, activation, and softmax layers make up CNN's educational process.

CNN is primarily composed of two phases: forward and backward propagation. Back-propagation methods are employed to enhance the parameters of the forward propagation algorithm. Link layers and several convolution layers are part of forward propagation. Convolution layers are layered on top of one another to extract various attributes from the input data. Low-level features are retrieved in the first feature extraction layer, while more complicated features are extracted in the following convolution layers. Furthermore, local linkages of features identified from earlier layers and mapped to particular feature maps of their data are assigned by convolution layers. The three convolutional layers have three batch normalizations, three rectifier linear units, or two max pooling layers and ReLUs. The network comprises three layers: completely connected, softmax, and classification once the three stages of convolution are completed. First, it is crucial to employ STFT to preprocess the training data.

3.4.2. Bilateral Long Short-Term Memory

An alternative to RNN called Bi-LSTM maintains long-term temporal relationships while avoiding the problem of an expanding gradient. The BiLSTM blocks are referred to as memory cells since they contain multiplicative gates like input, output, and forget gates. The input gate determines the current data rate that must be passed.

$$i_t = \sigma(P^i X_t + W^i b_t - 1) \quad (12)$$

The forget gate deliberates as it determines whatever data from the previous state has to be transferred,

$$f_t = \sigma(P^f X_t + W^f h_t - 1) \quad (13)$$

The output gate selects and expresses the internal state data that must be passed as,

$$o_t = \sigma(P^o X_t + W^o h_t - 1) \quad (14)$$

The unit c_t internal memory can be summed up as follows:

$$c_t = c_{t-1} \circ f_t + \hat{b} \circ i_t \quad (15)$$

Where \circ is the element-wise multiplication operator and c_{t-1} is the prior memory. The candidate's concealed state \hat{h} is assessed as,

$$\hat{h} = \tan h(P^b X_t + W^b h_t - 1) \quad (16)$$

Lastly, the hidden state output h_t is represented as,

$$h_t = \tan h(c_t) \circ O_t \quad (17)$$

The time series data was classified using 100 BiLSTM blocks in this instance. Because of the limitations of this architecture, generalization is accomplished through the use of a drop-out layer instead of a pooling layer. Lastly, a completely connected layer, a soft max layer, and a classification layer are added to produce the final result.

4. Results and Discussion

The proposed work utilizes an EEG dataset for emotion recognition, and only FFT data points are chosen to classify emotions. By choosing only the FFT data points, the study focuses on the frequency domain information extracted from the EEG signals to predict emotions. In the proposed emotion detection system, EEG data analyzed FFT to extract frequency domain features is utilized. EEG records electrical activity in the brain over time, and analyzing the frequency components can provide insights into different cognitive and emotional states. Figure 4 depicts the input EEG signal image which is to be processed.

Figure 5 displays the positive, negative, and neutral stages based on the input data. This implies that the figure visually represents the distinct states or categories, with positive likely denoting emotionally positive stages, negative indicating emotionally negative stages and neutral signifying periods with a lack of significant emotional intensity.

The EEG data undergoes preprocessing using a Gaussian Smoothing Filter to eliminate artifacts, as depicted in Figure 6. Gaussian Smoothing Filter serves as a crucial step in isolating intrinsic oscillatory components from the EEG data. This preprocessing step is crucial in refining the EEG data by reducing noise and unwanted distortions, enhancing the quality and reliability of the information.

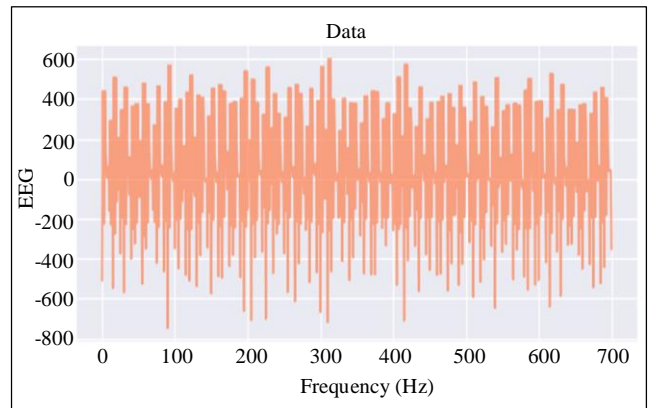


Fig. 4 Input EEG signal

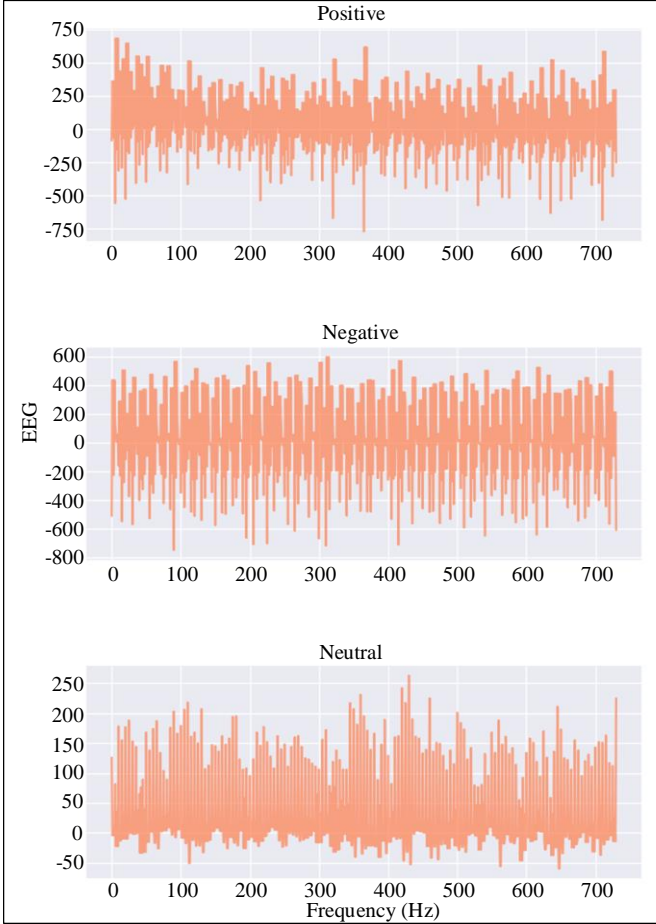


Fig. 5 Positive, negative, and neutral waveforms of the input EEG signal

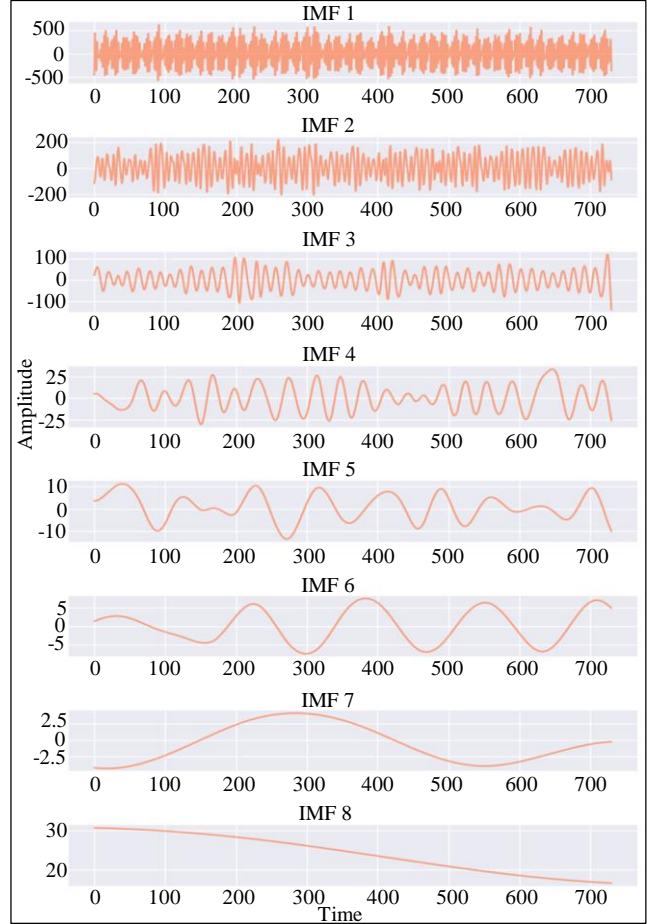


Fig. 7 Feature extraction with the EMD method

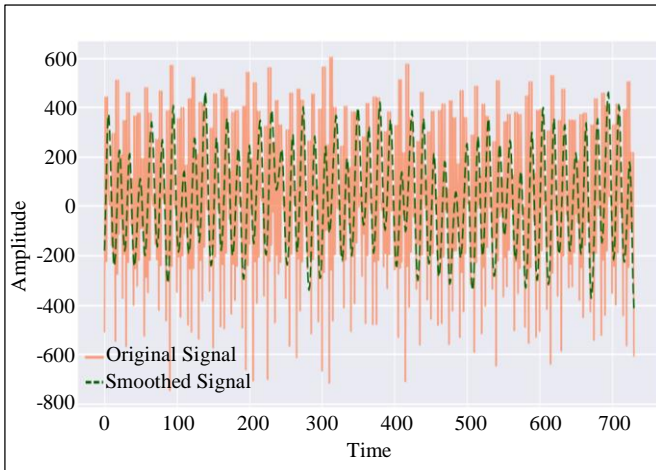


Fig. 6 Gaussian smoothing filter processing for artifact elimination

Following the initial preprocessing with the Gaussian Smoothing Filter, the data undergoes further refinement by implementing the EMD technique, represented in Figure 7. The results obtained through EMD capture distinct patterns related to emotional states.

These IMFs represent the underlying oscillatory modes of the EEG signal, providing a more granular and detailed representation of the emotional dynamics within the data. By decomposing the EEG signal into these intrinsic components, the EMD technique aids in extracting relevant features associated with various emotional states, contributing to the accuracy and sensitivity of the subsequent emotion detection system.

The next step in the process involves selecting optimal features employing the Gazelle-WOA algorithm, ensuring that the selected features contribute significantly to improving the accuracy and effectiveness of the emotion detection system.

The proposed Attention-Based Improved DCNN-BiLSTM model for accurately classifying emotions achieves a notable efficiency of 98.28%. Additionally, the model exhibits minimized loss, indicating that during its training process, the algorithm successfully optimized its parameters to minimize the difference between forecast and actual values, depicted in Figure 8.

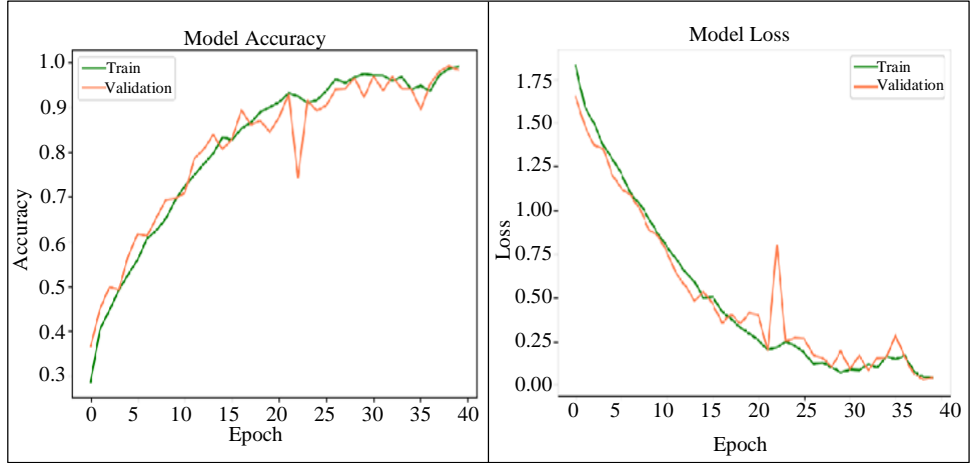


Fig. 8 Training and validation results of DCNN-BiLSTM with an attentional basis

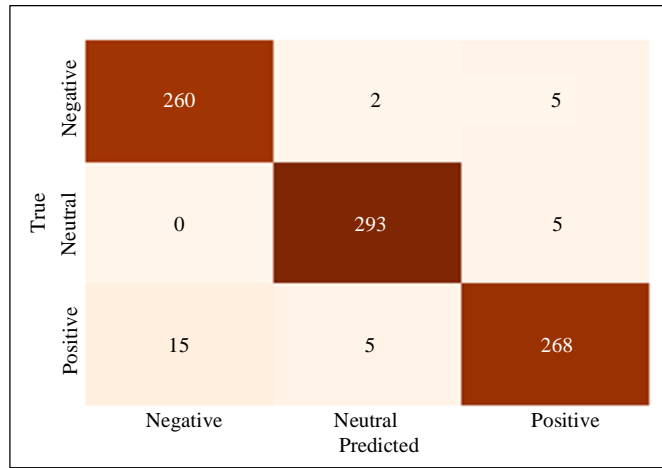


Fig. 9 Confusion matrix

Figure 9 represents the confusion matrix tested utilizing the dataset, depending on the identification results of mental state. This representation aids in assessing the model’s performance for each emotion class, positive, neutral, and negative, offering insights into accuracy, precision, and recall. A comparison analysis of the proposed DCNN-BiLSTM with other classifiers, such as SVM [25], CNN [26], and LSTM [27], is depicted in Table 2 also, the related graph is displayed

in Figure 10. The outcomes show that the developed improved classifier has an exceptional 98.28% accuracy rate in forecasting human emotions. The developed improved DCNN-BiLSTM is compared with other conventional classifiers to determine better performance metrics. From Table 3 and Figure 11, it is evident that the proposed improved classifier has enhanced recall, F1 score and precision than the other existing approaches.

Table 1. Comparison of classification strategy

Authors	Neural Network	Accuracy	Dataset Used
Arjun [21]	Attention Based CNN	72.3%	SEED, DEEP and CHB-MIT
Pragati Patel [5]	EMD	87.32%	DEEP
Wang [22]	CNN	94.96%	SEED and DEEP
Bazgir [23]	SVM, KNN and ANN	91.1%	DEAP
X.H Wang [24]	BDGLS+DE	93.7%	SEED
Proposed	Attention Based Improved DCNN-BiLSTM	98.28%	EEG Brainwave

Table 2. Accuracy comparison

Classifier	Accuracy (%)
SVM [25]	88
CNN [26]	93.01
LSTM [27]	87.25
Proposed Attention Based Improved DCNN-BiLSTM	98.28

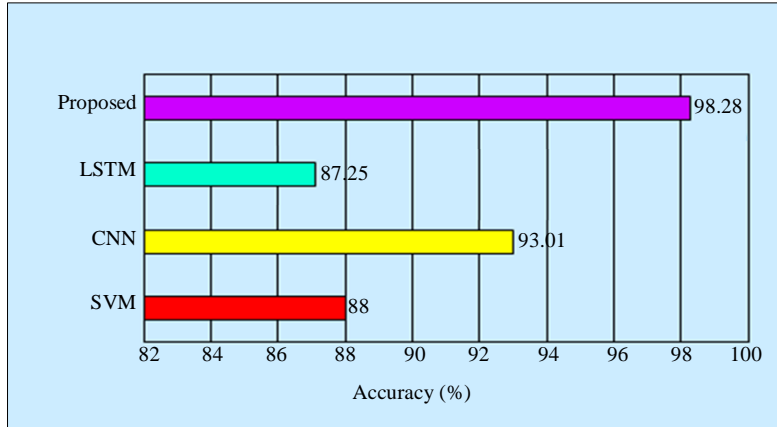


Fig. 10 Accuracy comparison

Table 3. Comparison of performance metrics for various classifiers

Approaches	Recall (%)	F1 Score (%)	Precision (%)
K-NN [28]	72	70	70
2D CNN [29]	91.02	93.32	92.89
RNN [2]	93	92	93
GRU [2]	95	95	95
Proposed Improved DCNN-BiLSTM	98.28	97.54	98.12

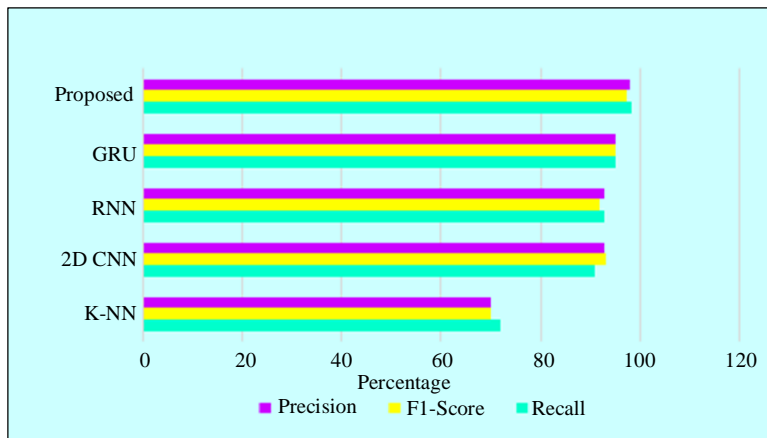


Fig. 11 Comparison of performance metrics for different classifiers

5. Conclusion

This work presents a comprehensive and advanced methodology for emotion recognition by utilizing EEG signals leveraging the power of DL techniques.

The proposed approach addresses the limitations of traditional methods by incorporating Gaussian smoothing filters for artifact reduction, EMD for feature extraction, and a hybrid Gazelle-Whale Optimization for optimal feature selection. Integrating Attention-based Improved DCNN-

BiLSTM networks for emotion classification results in improved accuracy of 98.28%. The overall proposed strategy is executed in Python software, and the comparative assessment is made over conventional topologies to illustrate the prominence of the implemented work.

Consequently, the comparison outcomes showed that the proposed improved DCNN-BiLSTM classifier achieved better performance indices and accuracy than the other existing topologies correspondingly.

References

- [1] Rania Alhalaseh, and Suzan Alasasfeh, "Machine-Learning-Based Emotion Recognition System Using EEG Signals," *Computers*, vol. 9, no. 4, pp. 1-15, 2020. [[CrossRef](#)] [[Google Scholar](#)] [[Publisher Link](#)]
- [2] M. Kalpana Chowdary, J. Anitha, and D. Jude Hemanth, "Emotion Recognition from EEG Signals Using Recurrent Neural Networks," *Electronics*, vol. 11, no. 15, pp. 1-20, 2022. [[CrossRef](#)] [[Google Scholar](#)] [[Publisher Link](#)]
- [3] Javier Marín-Morales et al., "Affective Computing in Virtual Reality: Emotion Recognition from Brain and Heartbeat Dynamics Using Wearable Sensors," *Scientific Reports*, vol. 8, no. 1, pp. 1-15, 2018. [[CrossRef](#)] [[Google Scholar](#)] [[Publisher Link](#)]
- [4] Murside Degirmenci et al., "Emotion Recognition from EEG Signals by Using Empirical Mode Decomposition," *2018 Medical Technologies National Congress (TIPTEKNO)*, Magusa, Cyprus, pp. 1-4, 2018. [[CrossRef](#)] [[Google Scholar](#)] [[Publisher Link](#)]
- [5] Pragati Patel, Raghunandan R., and Ramesh Naidu Annavarapu, "EEG-Based Human Emotion Recognition Using Entropy as a Feature Extraction Measure," *Brain Informatics*, vol. 8, pp. 1-13, 2021. [[CrossRef](#)] [[Google Scholar](#)] [[Publisher Link](#)]
- [6] Wei Li et al., "A Novel Spatio-Temporal Field for Emotion Recognition Based on EEG Signals," *IEEE Sensors Journal*, vol. 21, no. 23, pp. 26941-26950, 2021. [[CrossRef](#)] [[Google Scholar](#)] [[Publisher Link](#)]
- [7] Tran-Dac-Thinkh Phan et al., "EEG-Based Emotion Recognition by Convolutional Neural Network with Multi-Scale Kernels," *Sensors*, vol. 21, no. 15, pp. 1-13, 2021. [[CrossRef](#)] [[Google Scholar](#)] [[Publisher Link](#)]
- [8] Ahmed S. Eltrass, and Noha H. Ghanem, "A New Automated Multi-Stage System of Non-Local Means and Multi-Kernel Adaptive Filtering Techniques for EEG Noise and Artifacts Suppression," *Journal of Neural Engineering*, vol. 18, 2021. [[CrossRef](#)] [[Google Scholar](#)] [[Publisher Link](#)]
- [9] P.V.V.S. Srinivas, and Pragnyaban Mishra, "A Novel Framework for Facial Emotion Recognition with Noisy and de Noisy Techniques Applied in Data Pre-Processing," *International Journal of System Assurance Engineering and Management*, pp. 1-11, 2022. [[CrossRef](#)] [[Google Scholar](#)] [[Publisher Link](#)]
- [10] Haoshi Zhang et al., "A Robust Extraction Approach of Auditory Brainstem Response Using Adaptive Kalman Filtering Method," *IEEE Transactions on Biomedical Engineering*, vol. 69, no. 12, pp. 3792-3802, 2022. [[CrossRef](#)] [[Google Scholar](#)] [[Publisher Link](#)]
- [11] Souvik Phadikar, Nidul Sinha, and Rajdeep Ghosh, "Automatic Eyeblink Artifact Removal from EEG Signal Using Wavelet Transform with Heuristically Optimized Threshold," *IEEE Journal of Biomedical and Health Informatics*, vol. 25, no. 2, 475-484, 2020. [[CrossRef](#)] [[Google Scholar](#)] [[Publisher Link](#)]
- [12] Md. Rabiul Islam et al., "Emotion Recognition from EEG Signal Focusing on Deep Learning and Shallow Learning Techniques," *IEEE Access*, vol. 9, pp. 94601-94624, 2021. [[CrossRef](#)] [[Google Scholar](#)] [[Publisher Link](#)]
- [13] Patricia Becerra-Sánchez, Angelica Reyes-Munoz, and Antonio Guerrero-Ibañez, "Feature Selection Model Based on EEG Signals for Assessing the Cognitive Workload in Drivers," *Sensors*, vol. 20, no. 20, pp. 1-25, 2020. [[CrossRef](#)] [[Google Scholar](#)] [[Publisher Link](#)]
- [14] Yong Jiao et al., "Multi-View Multi-Scale Optimization of Feature Representation for EEG Classification Improvement," *IEEE Transactions on Neural Systems and Rehabilitation Engineering*, vol. 28, no. 12, pp. 2589-2597, 2020. [[CrossRef](#)] [[Google Scholar](#)] [[Publisher Link](#)]
- [15] Manosij Ghosh et al., "A Wrapper-Filter Feature Selection Technique Based on Ant Colony Optimization," *Neural Computing and Applications*, vol. 32, pp. 7839-7857, 2020. [[CrossRef](#)] [[Google Scholar](#)] [[Publisher Link](#)]
- [16] Min Li et al., "Computer-Aided Diagnosis and Staging of Pancreatic Cancer Based on CT Images," *IEEE Access*, vol. 8, pp. 141705-141718, 2020. [[CrossRef](#)] [[Google Scholar](#)] [[Publisher Link](#)]
- [17] Xiahan Chen et al., "Combined Spiral Transformation and Model-Driven Multi-Modal Deep Learning Scheme for Automatic Prediction of TP53 Mutation in Pancreatic Cancer," *IEEE Transactions on Medical Imaging*, vol. 40, no. 2, pp. 735-747, 2021. [[CrossRef](#)] [[Google Scholar](#)] [[Publisher Link](#)]
- [18] Xin Chai et al., "A Fast, Efficient Domain Adaptation Technique for Cross-Domain Electroencephalography (EEG)-Based Emotion Recognition," *Sensors*, vol. 17, no. 5, pp. 1-21, 2017. [[CrossRef](#)] [[Google Scholar](#)] [[Publisher Link](#)]

- [19] Jingxia Chen, Dongmei Jiang, and Yanning Zhang, "A Common Spatial Pattern and Wavelet Packet Decomposition Combined Method for EEG-Based Emotion Recognition," *Journal of Advanced Computational Intelligence and Intelligent Informatics*, vol. 23, no. 2, pp. 274-281, 2019. [[CrossRef](#)] [[Google Scholar](#)] [[Publisher Link](#)]
- [20] Heng Cui et al., "EEG-Based Emotion Recognition Using an End-to-End Regional-Asymmetric Convolutional Neural Network," *Knowledge-Based Systems*, vol. 205, 2020. [[CrossRef](#)] [[Google Scholar](#)] [[Publisher Link](#)]
- [21] Arjun, Aniket Singh Rajpoot, and Mahesh Raveendranatha Panicker, "Subject Independent Emotion Recognition Using EEG Signals Employing Attention Driven Neural Networks," *Biomedical Signal Processing and Control*, vol. 75, 2022. [[CrossRef](#)] [[Google Scholar](#)] [[Publisher Link](#)]
- [22] Yixin Wang et al., "EEG Based Emotion Recognition with Similarity Learning Network," *2019 41st Annual International Conference of the IEEE Engineering in Medicine and Biology Society (EMBC)*, Berlin, Germany, pp. 1209-1212, 2019. [[CrossRef](#)] [[Google Scholar](#)] [[Publisher Link](#)]
- [23] Omid Bazgir, Zeynab Mohammadi, and Seyed Amir Hassan Habibi, "Emotion Recognition with Machine Learning Using EEG Signals," *2018 25th National and 3rd International Iranian Conference on Biomedical Engineering (ICBME)*, Qom, Iran, pp. 29-30, 2019. [[CrossRef](#)] [[Google Scholar](#)] [[Publisher Link](#)]
- [24] Xue-han Wang et al., "EEG Emotion Recognition Using Dynamical Graph Convolutional Neural Networks and Broad Learning System," *2018 IEEE International Conference on Bioinformatics and Biomedicine (BIBM)*, Madrid, Spain, pp. 1240-1244, 2018. [[CrossRef](#)] [[Google Scholar](#)] [[Publisher Link](#)]
- [25] Smith K. Khare, and Varun Bajaj, "Time-Frequency Representation and Convolutional Neural Network-Based Emotion Recognition," *IEEE Transactions on Neural Networks and Learning Systems*, vol. 32, no. 7, pp. 2901-2909, 2021. [[CrossRef](#)] [[Google Scholar](#)] [[Publisher Link](#)]
- [26] Debarshi Nath et al., "A Comparative Study of Subject-Dependent and Subject-Independent Strategies for EEG-Based Emotion Recognition Using LSTM Network," *Proceedings of the 2020 the 4th International Conference on Compute and Data Analysis*, pp. 142-147, 2020. [[CrossRef](#)] [[Google Scholar](#)] [[Publisher Link](#)]
- [27] Aya Hassouneh, A.M. Mutawa, and M. Murugappan, "Development of a Real-Time Emotion Recognition System Using Facial Expressions and EEG Based on Machine Learning and Deep Neural Network Methods," *Informatics in Medicine Unlocked*, vol. 20, pp. 1-9, 2020. [[CrossRef](#)] [[Google Scholar](#)] [[Publisher Link](#)]
- [28] Shtwai Alsubai, "Emotion Detection Using Deep Normalized Attention-Based Neural Network and Modified-Random Forest," *Sensors*, vol. 23, no. 1, pp. 1-19, 2022. [[CrossRef](#)] [[Google Scholar](#)] [[Publisher Link](#)]
- [29] Aseel Mahmoud et al., "A CNN Approach for Emotion Recognition via EEG," *Symmetry*, vol. 15, no. 10, pp. 1-19, 2023. [[CrossRef](#)] [[Google Scholar](#)] [[Publisher Link](#)]